RESEARCH ARTICLE
doi: 10.2306/scienceasia1513-1874.2023.033

*ScienceAsia* 49 (2023): **437–444**

# Synthesis and comparison analysis of modified silica adsorbent and bismuth catalyst for removal of bisphenol A

**Shanmuga Kittappa**[a], **Shaliza Ibrahim**[b], **Nuruol Syuhadaa Mohd**[a,*]

[a] Department of Civil Engineering, Faculty of Engineering, Universiti Malaya, Kuala Lumpur 50603 Malaysia
[b] Institute of Ocean and Earth Sciences, Universiti Malaya, Kuala Lumpur 50603 Malaysia

*Corresponding author, e-mail: n_syuhadaa@um.edu.my

*Received 17 Jun 2022, Accepted 13 Mar 2023*
*Available online 15 May 2023*

**ABSTRACT**: A novel material, Tris coated magnetic nano structured adsorbent (T-MNSA) was synthesized using incipient wetness impregnation method for removal of bisphenol A (BPA). T-MNSA maximum adsorption capacity was 160 mg/g and sorption density was 0.078 mole BPA/mole of Tris. In addition, degradation using ultrasound assisted bismuth ferrite (BF) sono-catalyst was studied for removal and cost efficiency differences. The degradation results show a complete removal of BPA at condition of 0.10 g/l of BF, 100% power, and 72 kHz frequency. The mechanism study reveals that T-MNSA forms biomolecules and covalently attaches to BPA, but BF generates large amount of $H_2O_2$ molecules and breaks down BPA to non-toxic $CO_2$ and water. Cost analysis study reveals that T-MNSA is more economical than BF due to lower production and removal cost, almost ten times lower than degradation process using BF, and the material can be commercially produced in bulk quantities.

**KEYWORDS**: adsorption materials, sonocatalytic degradation, endocrine disrupting compounds, mechanism of BPA removal

## INTRODUCTION

Endocrine disrupting compounds (EDCs) were defined as exogenous substances or a mixture that modifies the function(s) of the endocrine system and causes adverse health effects in an intact organism or population [1]. Many papers have reported the presence of EDCs in water sources particularly for drinking purpose. Exposure to EDCs in water has been associated with adverse health effects. Fent et al has confirmed that EDCs even at very low concentrations as ppb to ppt level can cause serious health risks to living organisms. For instance, the effect in relation to fish reproduction is caused by feminization and masculinization of fish in the aquatic wildlife [2–4]. In this research, bisphenol A (BPA) has been selected as the model pollutant.

In the environment, BPA was released mainly by anthropogenic activities by humans. BPA was found in a very low concentration usually from nanograms to micrograms per litre in water. BPA is naturally degradable under aerobic condition but still exists in the surface water and aquatic organisms due to its slow biodegradation and good stability properties [5].

Among conventional treatment system, adsorption is the most desirable method due to its high yield, easy handling, and cost efficiency [6]. Furthermore, adsorption materials such as nano structured silica (NSA), activated carbon (AC), and iron oxide are readily available, widely used, and inexpensive [7–9]. New and innovative adsorbents with a higher sorption rate and capacity are preferred because they have a longer lifespan and are cost-efficient and reusable [10]. Regeneration and reusability are additional requirements, which enhance the sustainability and reduce the operational and maintenance costs [11].

Sonolysis is an energy-intensive treatment process that requires an ultrasound (US) generator to produce sound waves with the adjustment of frequency and power. The application of sono-catalyst optimizes the sonolysis process and may reduce the energy required to achieve maximum output. The acoustic cavitation effect (degradation) from ultrasonic irradiation forms micro bubbles that grow and collapse [12–14]. The formation and collapse of these micro bubbles produces an effect called sonoluminescence and hot spots with extensive amounts of heat (up to 5000 K) and high pressure (above 1000 atm) [15, 16]. This is followed by the compression of water molecules to form hydroxyl ($^{\cdot}OH$) and radical hydrogen species ($^{\cdot}H$) [17, 18]. The ($^{\cdot}OH$) radical is a strong and non-selective oxidant with the ability to decompose organic pollutants in the wastewater immediately [13, 19].

The cost analysis refers to the determination of expense in relation to synthesize and operation of a treatment system. These costs consist of direct costs such as materials, manpower, and energy. It is surprising to find that very limited literatures have focussed on the cost analysis of adsorbents and sono-catalyst. Only few studies have indicated that the materials synthesized were costly but did not provide any substantial cost details for removal of EDCs particularly [20, 21]. In this work, a cost analysis was performed using the typical parameters to determine the removal cost of BPA using adsorption and degradation.

## MATERIALS AND METHODS

### Synthesis of Tris coated magnetic nano structured adsorbent (T-MNSA)

#### *Materials for T-MNSA synthesis*

Iron (II) sulfate heptahydrate ($FeSO_4 \cdot 7\,H_2O$) and potassium permanganate ($KMnO_4$) were purchased from MERCK (Darmstadt, Germany) and used in the synthesis of nano-magnetite. Pluronic P123 ($EO_{20}PO_{70}EO_{20}$) and silicon dioxide ($SiO_2$) were obtained from Sigma-Aldrich (St. Louis, MO, USA) and R&M (Kuala Lumpur, Malaysia), respectively. Pharmaceutical grade (99.9% purity) BPA was purchased from Sigma-Aldrich. Tris (99.5%), 2-Amino-2-(hydroxymethyl) propane-1,3-diol, were purchased from Sigma-Aldrich.

#### *Synthesis process of T-MNSA*

A silica solution was prepared by dissolving 1 M of $SiO_2$ into 1 M NaOH and continuously stirred at 45 °C for 20 h [22]. Another suspension containing nano-magnetite was prepared separately. The nano-magnetite was synthesized using a modified method of Schwertmann and Comell [23]. Forty grams of $FeSO_4 \cdot 7\,H_2O$ was dissolved in 500 ml deionised water (DI) at room temperature. The solution was heated to 80 °C, and the alkaline solution was added slowly. Separately, the alkaline solution was prepared using 22.4 g NaOH and 3.3 g $KNO_3$ in 415 ml of DI water. The color of the solution changed from yellowish to dark purplish, and then to black. The solution was stirred at 80 °C for 1 h and then stirred overnight at room temperature around 25 °C. The precipitated nano-magnetite was obtained by centrifugation, followed by washing for several times with deionized water and later dried in an oven at 60 °C [24].

A predetermined mass (1 g) of nano-magnetite was added into the 60 ml acidic solution containing pore-templating agent Pluronic P123 (4.25 g) and hydrochloric acid (2 M). The suspension was heated at 45 °C for 2 h. Then, 30 ml of silicate solution was added into the 60 ml suspension containing nano-magnetite. The mixed solution was stirred at 200 rpm for 3 h. The mixture was stirred continuously at room temperature overnight and then transferred to an autoclaved container and aged at 90 °C for 20 h. The precipitated solid and liquid were centrifuged at 2,000 rpm, and the solution was decanted. The solids were washed with DI water and ethanol (50%) and dried at 60 °C for 24 h. The dried samples were calcined at 500 °C for 6 h using a Western furnace. This material is called magnetised nano structured silica adsorbent (MNSA).

MNSA was dried in the oven at 60 °C prior to the impregnation of Tris. Tris was impregnated into MNSA using a wetness impregnation method. One mmol of Tris was dissolved in 10 ml methanol and stirred for 1 h. This solution was added drop wise into 1 g of MNSA and mixed homogenously. The material is called as Tris coated magnetised nano structured silica adsorbent (MNSA), denoted as T-MNSA. The molar ratio of the material was calculated based on the amount of Tris incorporated in one gram of MNSA and divided by the molecular weight of each compound. The T-MNSA synthesis ratio determine was 0.14 $Fe_3O_4$: 1 $SiO_2$: 1 NaOH: 0.1 HCl: 0.013 Pluronic: 167 $H_2O$: 0.001 Tris.

### Synthesis of bismuth ferrite (BF) catalyst

#### *Materials for BF sono-catalyst synthesis*

Bismuth nitrate pentahydrate ($Bi(NO_3)_3 \cdot 5\,H_2O$) was purchased from Sigma-Aldrich. Iron (II) nitrate heptahydrate ($Fe(NO)_3 \cdot 7\,H_2O$), BPA, methanol, absolute alcohol, and ethylene glycol were bought from MERCK. All chemicals were of analytical grade and used without any modification or purification. Laboratory DI was used for the preparation of all solutions.

#### *Synthesis process of BF*

Bismuth nitrate was accurately weighed (8 mmol) and dissolved in ethylene glycol and sonicated for 15 min. Stoichiometric proportion of $Fe(NO)_3 \cdot 7\,H_2O$ was added into the solution and sonicated for another 20 min to obtain a brown reddish solution. The mixture was then transferred into a Teflon autoclave and stored in the oven at 80 °C for 8 h to form a xenogel, a solid-liquid gel state. The xenogel was transferred to a crucible and calcined at 400 °C for 1.5 h. The calcinated powder was transferred to a vacuum filter apparatus, washed with water and absolute alcohol for several times, and finally was dried in the oven at 70 °C overnight.

### Removal of BPA via adsorption using T-MNSA

The removal of BPA by T-MNSA was investigated via series of kinetic experiments. In a conical flask, 50 mg of T-MNSA was added into 200 ml solution containing BPA (0.25 g/l dosage). Then, the solution was shaken at 200 rpm for 8 h using an orbital shaker. The solution and adsorbent were separated using a simple laboratory magnet to remove the adsorbent from the solution. The solution was tested for the remaining BPA in the solution.

### Removal of BPA via ultrasound degradation using BF

The degradation of BPA was analyzed using 2 sets of data: a blank solution and a sample of 5.0 mg/l BPA solution in ultrasound without BF sono-catalyst. The amount of $H_2O_2$ generated was determined using KI dosimetry method and UV-vis spectroscopy. The effects of BF catalyst addition on degradation of BPA by ultrasound was assessed by adding 0.05 g/l of BF catalyst into the 1 l BPA solution prior to the US

treatment. Then, 8 ml of sample was taken every 10 min until 1 h. The sample was calibrated with KI dosimetry method and tested with UV-vis for the absorbance value. The result was compared with BPA degradation by US without adding of BF catalyst. The sonification analysis was done using a customize ultrasound sonicator. Different concentrations (0.10 g/l and 0.20 g/l) of BF were added into the BPA solution to determine the concentration of BF catalyst that is required to remove BPA from water. Other parameters such as ultrasound frequencies (72 kHz), applied ultrasound powers (50%), and temperatures ($25 \pm 1$ °C) were maintained constant, and the experiments were repeated.

### Cost analysis

The cost analysis was performed based on 3 major factors: materials, energy, and manpower. The material cost determination was done using the main materials and chemicals utilized in the synthesis of the adsorbents and sono-catalysts. The price of silica was around RM 5.60 per kg. Bismuth and iron nitride were laboratory grade (purity above 95%) chemicals purchased at RM 1.00 per gram for bismuth and RM 0.52 per gram for iron nitride. Energy consumption was determined by taking into consideration only the major equipment applied in this work. The standard calculation of energy was based on the formula: E(energy) kWh = (power (Watt) × H (hours of usage)/1000). Major electrical equipment was taken into consideration including hot plates, oven, furnace, shaker, stirrer, and ultrasound reactor in the energy determination process. Electricity price was RM 0.435/kWh; the tariff rate by Tenaga Nasional Malaysia for industrial customers was used to determine the energy cost.

The manpower cost was calculated by estimating number of hours spent by a person to complete the synthesis and removal by either adsorption or degradation. It is assumed that this task was performed by a technician or an executive level staff with salary of around RM 3000 per month. Based on 8 hours of work and 26 days a month, per hour salary (manpower cost) will be RM 14.42. This value RM 14.42 was multiplied by the number of hours estimated for each task to be completed to calculate the manpower cost.

## RESULTS AND DISCUSSION

### Physical properties of T-MNSA

$N_2$ gas adsorption and desorption results in Fig. 1A shows that MNSA available surface area is $5.76 \times 10^{20}$ nm$^2$ (576 m$^2$/g) determined using Brunauer-Emmett-Teller (BET) measurement technique. Three mmol Tris was coated into MNSA via an incipient wetness impregnation method to ensure that all molecules of Tris are well incorporated to form T-MNSA. Based on the acid-base back titration method, a molecule of Tris can occupy 2.88 nm$^2$ of surface of nano-$SiO_2$ [25]. This was used to interpret that a molecule of Tris

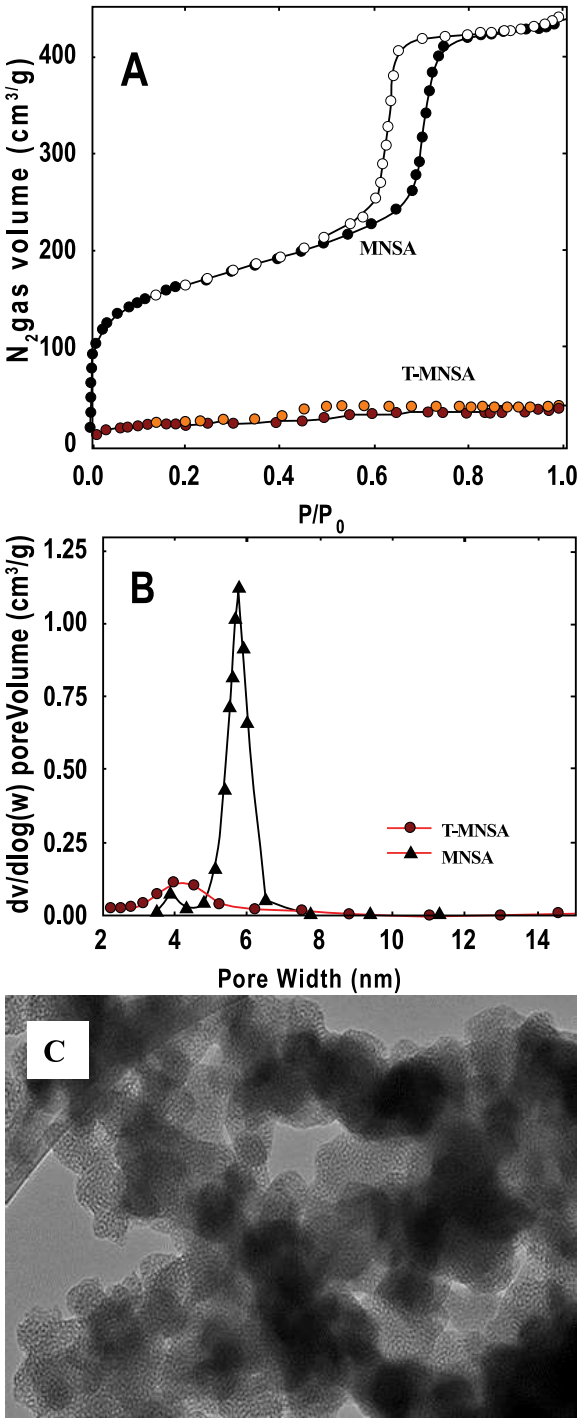


**Fig. 1** (A) BET surface area, (B) BJH pore size distribution of MNSA and T-MNSA, and (C) TEM image of T-MNSA.

occupied 0.96 $nm^2$ surface area of T-MNSA, deducing that the pore structure of T-MNSA was supersaturated with 3 mmol of Tris. After the incorporation of Tris, T-MNSA surface area was reduced to 42.2 $m^2/g$, pore volume matched with the IUPAC hysteresis loop Type IV H2 as shown in Fig. 1A [26].

The mean Barrett-Joyner-Halenda (BJH) desorption (Fig. 1B) shows that the pore diameter of MNSA was 6 nm and reduced to 4 nm after the incorporation of Tris (T-MNSA). This reduction in diameter is a result of silicate condensation during calcination via the incorporation of Tris [27]. T-MNSA could have lower thermal stability (up to 600 °C), which is due to the formation of weaker bonds between the condensed silica walls. TEM image in Fig. 1C reveals the formation of a homogenous surface of T-MNSA. The darker cloudy area seen in the TEM images observed was due to the impregnation of nano-magnetite into the adsorbent. The pores of T-MNSA are homogenous, which enhance the adsorption process of the adsorbate.

### Physical properties of BF adsorbent

X-ray diffraction analysis was performed to determine the phase composition of BF sono-catalyst. The XRD pattern and matching peaks (Fig. 2A) were matched using 2 standard reference compounds: bismuth ferrite (III) (ICSD Code: 245827) and bismuth oxide (ICSD Code: 417638). The results show that the BF sono-catalyst has matching peaks with the bismuth ferrite and bismuth oxide standards. The presence of bismuth oxide peak impurities was due to slow quenching process of the material at room temperature. The XRD matching peaks revealed that the BF forms a hexagonal structure with space group type R3c obtained from the standard reference [28]. Diffraction peak of (1 1 0) was selected as reference for the lattice space constant determination of BF. The d-spacing value determined from the XRD data is 3.96382 Å.

The physical and chemical properties of BF were further analyzed using field emission scanning electron microscopy (FESEM) and energy dispersive spectroscopy (EDS) that were performed at working voltage between 1–5 kV (Fig. 2B and C). The BF surface is homogenous, and it is compactly packed with uniform particle size. The red box is the selected area for the EDS elemental analysis. Two spots were chosen for the EDS analysis at working voltage of 10 kV. The EDS analysis (Fig. 2C) results indicated that the elemental ratio of Bi, Fe, and O in the BF nanoparticles is 1:1:3, which suggests the molecular formula as $BiFeO_3$. The production of small crystallite size of BF nanoparticles in this work could be due to the faster nucleation rate than the crystal growth itself during the ultrasound process. This finding demonstrates that ultrasound is a suitable method for preparing BF particles in nanoscale with uniform distribution of particles [29].

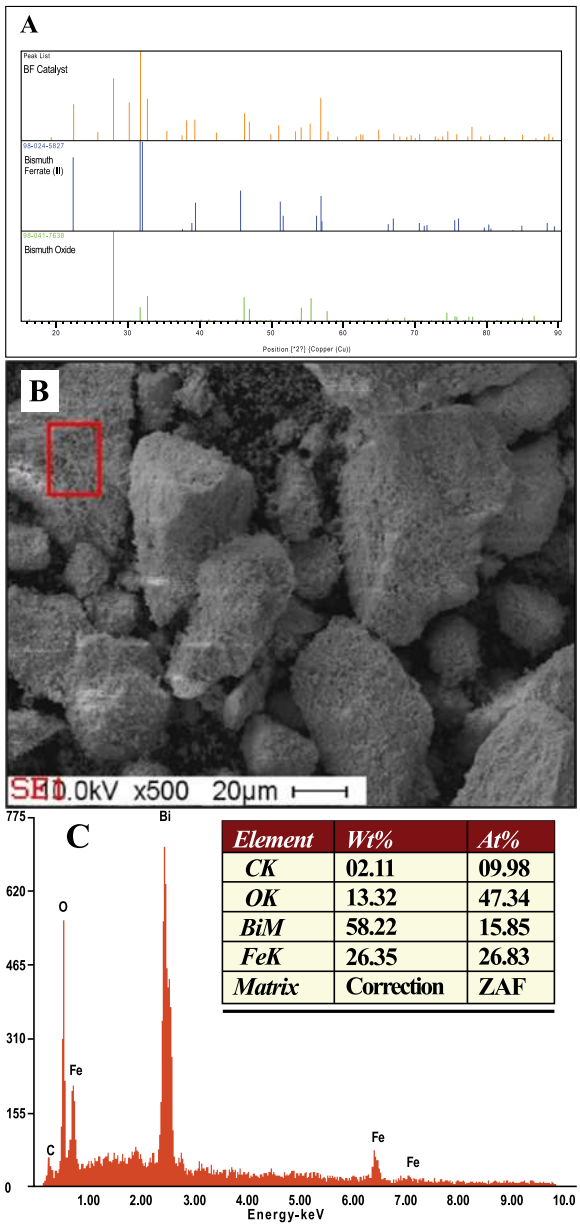


**Fig. 2** (A) XRD peaks of BF catalyst and reference patterns, (B) FESEM, and (C) EDS images of BF.

### Adsorption of BPA using T-MNSA

The kinetics of BPA removal by T-MNSA was investigated (Fig. 3). MNSA presents smaller adsorption capacity for BPA compared to T-MNSA. The equilibrium time required to reach plateau was around 300 min with adsorption capacity reaching up to 160 mg/g. The adsorption data was fitted with the pseudo 2nd order kinetic model with $R^2$ value of 0.991, signifying that the removal of BPA is a heterogeneous adsorption. The sorption density was 0.078 mole BPA/mole N of T-MNSA.

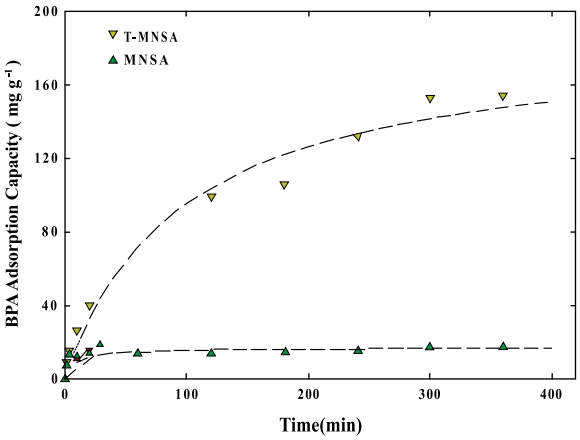


**Fig. 3** Time resolved uptake of BPA by MNSA and T-MNSA matching pseudo second order model.

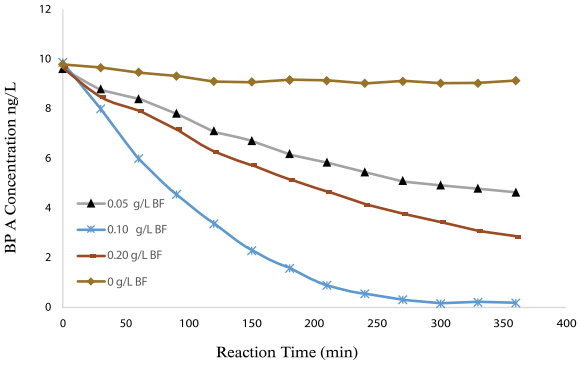


**Fig. 4** BPA degradation using BF at different concentrations.

The adsorption of BPA by T-MNSA shows higher capacity than that of MCM-41 and SBA-15 (nano structured silica adsorbents), commercial activated carbon (CAC) [30, 31], and fruit shell activated carbon [32, 33]. The MNSA without any functionalization demonstrated much lower adsorption capacity for BPA (Fig. 3). This result shows that surface modification and functionalization of adsorbent with TRIS improved the adsorption capacity of T-MNSA.

### Degradation of BPA using BF sono-catalyst

The determination of optimum condition of sono-catalyst required for the degradation of BPA was performed using different amounts of BF catalyst (Fig. 4). It was observed that the addition of BF sono-catalyst (0.05–0.20 g/l) reduced the concentration of BPA in the solution compared to the condition without the BF catalyst. The BF concentration of 0.10 g/l, 100% power, and 72 kHz frequency yielded the maximum removal of BPA, and further increase of catalyst did not increase the degradation of BPA as shown in Fig. 4. The generation of hydrogen peroxide ($H_2O_2$) during the degradation was measured, and the results show

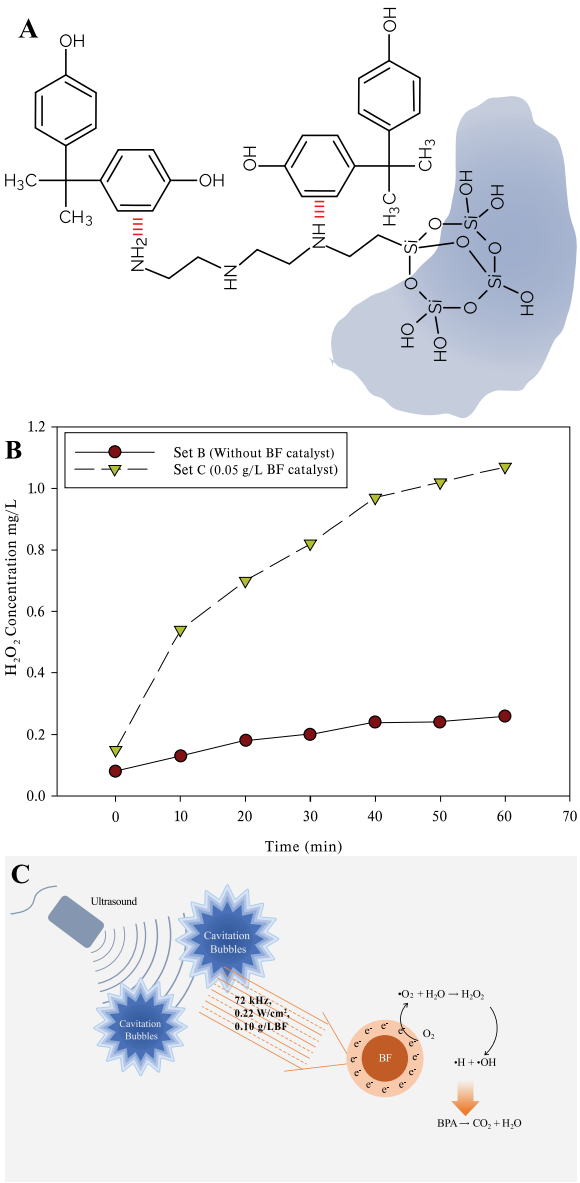


**Fig. 5** (A) Adsorption of BPA with T-MNSA. (B) The increase in $H_2O_2$ concentration with the addition of BF catalyst. (C) Ultrasound degradation mechanism.

that the increase of the BF catalyst increases the production of $H_2O_2$ until it reaches maximum production at 0.10 g/l.

### Comparison of adsorption and degradation mechanism of BPA removal

The incorporation of Tris into MNSA has enhanced its removal capacity and adsorption rate significantly. Adsorption of T-MNSA with BPA leads to formation of biomolecules [34]. These biomolecules are active and able to covalently attach to the pollutant. There

is possible exchange of electrons and ions during the interaction of biomolecules and BPA. The biomolecules may form hydrogen bonding with the amine group of T-MNSA as shown in Fig. 5A. The formation of biomolecule and bonding indicates that chemisorption is more prevailing than physical sorption. The proposed mechanism here has similarities with the adsorption of earlier reported work of carbon nano tubes, mesoporous silica, and activated carbon [5, 7, 24] with protein and enzyme [35].

The experimental data show that the BF has assisted the degradation of BPA via producing high intensity ultrasound activity causing rapid increase of $H_2O_2$ concentration in the solution (Fig. 5B). The increase in frequency (72 kHz) and power (100%) enhanced the acoustic cavitation, which subsequently improved the sonocatalytic activity in the solution [35]. To achieve high ultrasound activity, rapid production of collapsing bubbles, which can generate high local transitory temperature and pressure, is required [36]. The addition of BF sono-catalyst enhanced the acoustic cavitation through a chemical influence termed as chemical-sonocatalytic effect (Fig. 5C) [37]. According to Soltani & Entezari, the chemical sonocatalytic impact can only take place if the energy supplied is above the required band gap energy, enabling the degradation process to occur [38]. In this case, high amount of $H_2O_2$ molecules broke down to free radicals, which dissociate the BPA molecules and decompose them to $CO_2$ and $H_2O$ (Fig. 5B).

### Economic consideration

The material cost was calculated based on the raw material prices and amount of materials and chemicals used for the synthesis of adsorbents and sono-catalyst. The calculated values show that total material cost per gram for synthesis of adsorbent was RM 0.72 for T-MNSA and RM 5.64 for BF sono-catalyst (RM 1 = USD 0.23). The energy cost for T-MNSA adsorption was RM 0.91 per gram, while cost for degradation was higher for BF (RM 3.13). Nevertheless, it was important to note that the sono-catalyst amount used for degradation was much lower (0.10 g) when compared with adsorption (1 g). The manpower cost was higher for treatment by BF compared to that of T-MNSA. The difference in the cost per gram is due to the amount of the yield produced; BF sono-catalyst produced was 0.84 g almost ten times lower compared to T-MNSA, which was 7.22 g.

### Cost efficiency analysis

The comparison analysis in this section focusses on both adsorbents and sono-catalysts that were used for removing BPA. By applying all 3 main parameters: raw material, energy, and manpower, the total cost ascertained was RM 74.24 per gram of BF and RM 12.35 per gram of T-MNSA (Table 1). The comparison of cost efficiency was performed based on the removal capacity and cost incurred.

**Table 1** Total removal costs using adsorption and degradation[†].

| Material | Raw material cost (RM) | Energy cost (RM) | Manpower cost (RM) | Total cost (RM) |
|---|---|---|---|---|
| T-MNSA | 0.72 | 1.43 | 10.20 | 12.35 |
| BF | 5.64 | 3.57 | 65.03 | 74.24 |

[†] Per gram synthesis of material.

**Table 2** Comparison of removal cost efficiency.

| Adsorbent/ Catalyst | Pollutant | RC[*] (mg/g) | Total cost (RM/g) | RCE[*] (mg/RM × 100) |
|---|---|---|---|---|
| T-MNSA | BPA | 4.72 | 12.35 | 38.53 |
| BF | BPA | 1.50 | 74.24 | 2.021 |

[*] RC = Removal Capacity (Qeq), RCE = Removal Cost Efficiency.

The values in Table 2 signified that each gram of T-MNSA can remove 4.72 mg of BPA from the solution at the cost of RM 12.35. This is lower compared to the cost of using BF when each gram can remove 1.50 g of BPA at the cost of RM 74.24. In terms of cost efficiency, T-MNSA is 20 times cheaper than BF sono-catalyst. Therefore, in terms of practical application, T-MNSA is more capable of treating higher volume of polluted waters with the same concentration of pollutant.

The synthesis costs for all materials studied in this work can be further lowered if the equipment was used at full capacity. For instance, in energy consumption determination, many of the equipment that were used for synthesis have high-capacity usage. However, the capacity of the equipment was underutilized. In the actual manufacturing scenario, the cost will be much lower because the equipment will be used at maximum capacity, unlike in the laboratory. Furthermore, all calculations were based on the chemicals that were of analytical grade. In an industrial manufacturing setting, all these materials will be able to produce in bulk using industrial grade chemicals, which are much cheaper than the analytical grade.

## CONCLUSION

BF sono-catalyst and T-MNSA were produced via low energy synthesis routes. Both materials were able to assist in removing the BPA from solution, indicating their suitable application in water purification process. T-MNSA exhibited high adsorption capacity for BPA, almost 4 times more than intermediate adsorbent MNSA without Tris, whereas BF was able to remove 100% of BPA within a short period depending on the concentration of the catalyst. The modified T-MNSA has been proven to have higher adsorption capacity and better

binding affinity for BPA, and hence has improved the removal of BPA. The BF, on the other hand, produced free radicals and electrons that eventually increased the amount of $H_2O_2$ in the solution and degraded the BPA. The cost analysis study revealed that T-MNSA is the best material for removing BPA compared to BF. BF is considered compliance as it can degrade BPA quickly.

*Acknowledgements*: We would like to express our special gratitude to Universiti Malaya for providing financial aid for the research project (grant numbers RP008C-14SUS), which covers the research work and the related expenses.

## REFERENCES

1. Organization WH (2002) IPCS global assessment of the state-of-the-science of endocrine disruptors. *Who/Pcs/Edc/02* **2**, 35–50.
2. Tsutsumi O (2005) Assessment of human contamination of estrogenic endocrine-disrupting chemicals and their risk for human reproduction. *J Steroid Biochem* **93**, 325–330.
3. McLachlan JA, Simpson E, Martin M (2006) Endocrine disrupters and female reproductive health. *Best Pract Res Clin Endocrinol Metab* **20**, 63–75.
4. Jermann D, Pronk W, Bollerc M, Schäfer AI (2009) The role of NOM fouling for the retention of estradiol and ibuprofen during ultrafiltration. *J Membrane Sci* **329**, 75–84.
5. Kim YH, Lee B, Choo KH, Choi SJ (2011) Selective adsorption of bisphenol A by organic-inorganic hybrid mesoporous silicas. *Micropor Mesopor Mat* **138**, 184–190.
6. Zare K, Sadegh H, Shahryari-Ghoshekandi R, Maazinejad B, Ali V, Tyagi I, Gupta VK (2015) Enhanced removal of toxic Congo red dye using multi walled carbon nanotubes: kinetic, equilibrium studies and its comparison with other adsorbents. *J Mol Liq* **212**, 266–271.
7. Khanday WA, Marrakchi F, Asif M, Hameed BH (2017) Mesoporous zeolite-activated carbon composite from oil palm ash as an effective adsorbent for methylene blue. *J Taiwan Inst Chem E* **70**, 32–41.
8. Tan I, Hameed B, Ahmad A(2007) Equilibrium and kinetic studies on basic dye adsorption by oil palm fibre activated carbon. *Chem Eng J* **127**, 111–119.
9. Imamoglu M, Tekir O (2008) Removal of copper (II) and lead (II) ions from aqueous solutions by adsorption on activated carbon from a new precursor hazelnut husks. *Desalination* **228**, 108–113.
10. Sirival R, Patdhanagul N, Preecharram S, Saikhao L (2021) Removal of 2,4-dichlorophenoxyacetic acid from water by modified zeolite adsorbents. *ScienceAsia* **47**, 602–608.
11. Sun Q, Wang Y, Li L, Bing J, Wang Y, Yan H (2015) Mechanism for enhanced degradation of clofibric acid in aqueous by catalytic ozonation over $MnO_x$/SBA-15. *J Hazard Mater* **286**,276–284.
12. Cai MQ, Wei XQ, Song ZJ, Jin MC (2015) Decolorization of azo dye Orange G by aluminum powder enhanced by ultrasonic irradiation. *Ultrason Sonochem* **22**, 167–173.
13. Mahvi A (2009) Application of ultrasonic technology for water and wastewater treatment. *Iran J Public Health* **38**, 1–17.
14. Chang Q, Zhu L, Luo Z, Lei M, Zhang S, Tang H (2011) Sono-assisted preparation of magnetic magnesium-aluminum layered double hydroxides and their application for removing fluoride. *Ultrason Sonochem* **18**, 553–561.vfill
15. He LL, Liu XP, Wang YX, Wang ZX, Yang YJ, Gao YP, Wang X (2016) Sonochemical degradation of methyl orange in the presence of $Bi_2WO_6$: Effect of operating parameters and the generated reactive oxygen species. *Ultrason Sonochem* **33**, 90–98.
16. Wu CH (2007) Sonocatalytic degradation of C.I. Reactive Red 198 in $H_2O_2$-based Systems. *React Kinet Catal L* **92**, 377–384.
17. Wang J, Lv Y, Zhang Z, Deng Y, Zhang L, Liu B, Zhang X (2009) Sonocatalytic degradation of azo fuchsine in the presence of the Co-doped and Cr-doped mixed crystal $TiO_2$ powders and comparison of their sonocatalytic activities. *J Hazard Mater* **170**, 398–404.
18. Suslick KS (1989) The chemical effects of ultrasound. *Sci Am* **260**, 80–86.
19. Li P, Song Y, Wang S, Tao Z, Yu S, Liu Y (2015) Enhanced decolorization of methyl orange using zero-valent copper nanoparticles under assistance of hydrodynamic cavitation. *Ultrason Sonochem* **22**, 132–138.
20. Parshetti GK, Chowdhury S, Balasubramanian R (2015) Biomass derived low-cost microporous adsorbents for efficient $CO_2$ capture. *Fuel* **148**, 246–254.
21. Gkika DA, Liakos EV, Vordos N, Kontogoulidou C, Magafas L, Bikiaris DN, Kyzas GZ (2019) Cost estimation of polymeric adsorbents. *Polymers Basel* **11**, 925.
22. Chaudhary V (2018) Synthesis and catalytic activity of SBA-15 supported catalysts for styrene oxidation. *Chin J Chem Eng* **26**, 1300–1306.
23. Cornell RM, Schwertmann U (2006) *The Iron Oxides: Structure, Properties, Reactions, Occurrences and Uses*, Vol 664, John Wiley & Sons.
24. Kittappa S, Pichiah S, Kim JR, Yoon Y, Snyder SA, Jang M (2015) Magnetised nanocomposite mesoporous silica and its application for effective removal of methylene blue from aqueous solution. *Sep Purif Technol* **153**, 67–75.
25. Jung HS, Moon DS, Lee JK (2012) Quantitative analysis and efficient surface modification of silica nanoparticles. *J Nanomater* **2012**, 593471.
26. Choma J, Jaroniec M (2006) Characterization of nanoporous carbons by using gas adsorption isotherms. *Interface Sci Technol* **7**, 107–158.
27. Zhao D, Huo Q, Feng J, Chmelka BF, Stucky GD (1998) Nonionic triblock and star diblock copolymer and oligomeric surfactant syntheses of highly ordered, hydrothermally stable, mesoporous silica structures. *J Am Chem Soc* **120**, 6024–6036.
28. Kothari D, Reddy VR, Sathe VG, Gupta A, Banerjee A, Awasthi AM (2008) Raman scattering study of polycrystalline magnetoelectric $BiFeO_3$. *J Magn Magn Mater* **320**, 548–552.
29. Yoon M, Seo M, Jeong C, Jang JH, Jeon KS (2005) Synthesis of liposome-templated titania nanodisks: optical properties and photocatalytic activities. *Chem Mater* **17**, 6069–6079.
30. Bui TX, Choi H (2009) Adsorptive removal of selected pharmaceuticals by mesoporous silica SBA-15. *J Hazard Mater* **168**, 602–608.

31. Baccar R, Sarrà M, Bouzid J, Feki M, Blánquez P (2012) Removal of pharmaceutical compounds by activated carbon prepared from agricultural by-product. *Chem Eng J* **211**, 310–317.
32. Sivarajasekar N, Mohanraj N, Balasubramani K, Prakash Maran J, Ganesh Moorthy I, Karthik V, Karthikeyan K (2017) Optimization, equilibrium and kinetic studies on ibuprofen removal onto microwave assisted-activated *Aegle marmelos correa* fruit shell. *Desalin Water Treat* **84**, 48–58.
33. Hernández-Abreu AB, Àlvarez-Torrellas S, Águeda VI, Larriba M, Delgado JA, Calvo PA, García J (2020) Enhanced removal of the endocrine disruptor compound Bisphenol A by adsorption onto green-carbon materials. Effect of real effluents on the adsorption process. *J Environ Manage* **266**, 110604.
34. Quan X, Liu J, Zhou J (2019) Multiscale modeling and simulations of protein adsorption: progresses and perspectives. *Curr Opin Colloid Interface Sci* **41**, 74–85.
35. Gholami P, Dinpazhoh L, Khataee A, Orooji Y (2019) Sonocatalytic activity of biochar-supported ZnO nanorods in degradation of gemifloxacin: synergy study, effect of parameters and phytotoxicity evaluation. *Ultrason Sonochem* **55**, 44–56.
36. Lee G, Chu KH, Al-Hamadani YA, Park CM, Jang M, Heo J, Yoon Y (2018) Fabrication of graphene-oxide/β-$Bi_2O_3$/$TiO_2$/$Bi_2Ti_2O_7$ heterojuncted nanocomposite and its sonocatalytic degradation for selected pharmaceuticals. *Chemosphere* **212**, 723–733.
37. Jun BM, Kim S, Heo J, Her N, Jang M, Park CM, Yoon Y (2019) Enhanced sonocatalytic degradation of carbamazepine and salicylic acid using a metal-organic framework. *Ultrason Sonochem* **56**, 174–182.
38. Soltani T, Entezari MH (2014) Solar-Fenton catalytic degradation of phenolic compounds by impure bismuth ferrite nanoparticles synthesized via ultrasound. *Chem Eng J* **251**, 207–216.